A MODELING APPROACH FOR STUDYING FOREST CHLOROPHYLL CONTENT IN RELATION TO CANOPY COMPOSITION

J. Verrelst [a, *], M.E. Schaepman [a], J.G.P.W. Clevers [a]

[a]Centre for Geo-Information, Wageningen UR, Wageningen, The Netherlands – (Jochem.Verrelst, Michael.Schaepman, Jan.Clevers)@wur.nl

Commission VII, WG VII/1

KEY WORDS: Chlorophyll Content, Non-Photosynthetic Vegetation, PROSPECT, FLIGHT, Canopy Structure, Woody Elements

ABSTRACT:

Foliar concentration of the main photosynthetic pigments chlorophyll *a* and *b* (*Cab*) is widely regarded as a generic bioindicator of the actual plant status. However, when the scale moves up to stand level, relationships between the spectral response and leaf chemistry tend to break down due to confounding factors such as canopy structure, woody elements and background contributions. Especially in old-growth forests large numbers of standing and fallen dead wood are generated. We questioned the role of woody elements in the retrieval of *Cab* content on the basis of synthetic reflectance data through coupling of leaf-level (PROSPECT) and canopy-level (FLIGHT) radiative transfer models. For a wide range of forest stands the *Cab*-induced dispersion (Coefficient of Variation: CV_{Cab}) and total spread (Standard Deviation: SD) was calculated. The magnitude of CV_{Cab} and SD provides information about the *Cab*-related spectral spread and can therefore be regarded as stand-specific indicators of the theoretical *Cab* detectability. Results demonstrate that in dense canopies woody elements are key players in suppressing the *Cab*-related spectral spread. Apart from composition canopy structure also exerts influence: e.g. an overstory with crown coverage (CC) of 60% and a crown LAI of 1.5 propagated greatest spectral spread. In sparse stands (e.g. CC<40%) the background contribution is the dominant confounding factor. The impact that woody elements exert in the theoretical retrieval of *Cab* content was quantified for four distinct real-world coniferous forest types.

1. INTRODUCTION

Foliar concentration of the main photosynthetic pigments chlorophyll *a* and *b* (*Cab*) is widely regarded as a generic bioindicator of the actual plant status, such as stress condition (Lichtenthaler et al., 1996) and vegetation gross primary productivity (Gitelson et al., 2006). Various leaf and canopy experiments have indicated that imaging spectroscopy is a potentially powerful tool for assessing variation in chlorophyll content of trees (Ustin et al., 2004). However, when the scale moves up to stand or landscape level, relationships between the reflected electromagnetic radiation and leaf chemistry tend to break down (e.g. Trotter et al., 2002). Then the subtle scattering and absorption properties of the foliar chemistry are confounded by whole-tree features such as the foliage structural arrangement, woody elements and background reflectances (e.g. Asner, 1998).

At landscape level, a common approach to deal with sub-pixel complexity is to unmix a pixel into its most distinct, 'pure' endmembers. For instance, a vegetated surface might be decomposed into fractions of photosynthetic vegetation (PV), non-photosynthetic vegetation (NPV) and bare soil. Although pixel unmixing into NPV-PV-bare soil endmembers facilitated to study ecosystem dynamics (e.g. Asner et al., 2004; Jia et al., 2006), it does not provide understanding of the true complexity between the interaction of phytoelements and radiant energy. Alternatively, leaf chemistry estimates retrieved from optical remote sensing can be investigated using radiative transfer models, which describe the transfer and interaction of solar radiation inside the canopy based on physical laws and thus provide an explicit connection between the phytoelements and the canopy reflectance. While much work exists in the realm of radiate transfer modeling, the relative importance of woody elements (NPV) in the context of quantifying canopy chlorophyll content however has not adequately been evaluated. Only recently the influence of the 3D structure of trunks and branches in a coniferous canopy on reflectance has been explicitly quantified (Malenovsky et al., 2008). Yet this work comprised a young production forest (e.g. <30 year), where woody elements are exclusively part of the standing trees and concentrated in the lower part of the canopy. By contrast, in old-growth forests a surplus of woody parts in the form of lying and standing deadwood are scattered within the canopy layer and on the forest floor and can encompass 18-40% of total woody biomass (Siitonen 2001). In these older forests woody parts play a significant role in determining canopy reflectance (Asner, 1998), as they are an important photon absorbing and scattering component. Apart from changing canopy composition, the forest also increases in heterogeneity during aging (Franklin et al., 2002); making structural attributes equally important drivers of the canopy spectral response (Song et al., 2002). This paper reports on the propagation of canopy compositional and structural effects when inferring chlorophyll content assessments on the basis of synthetic reflectance data. We used the leaf-level model PROSPECT (Jacquemoud et al., 1996) coupled with the canopy-level ray-tracing model FLIGHT (North, 1996). The coupled models allow controlling simultaneously foliar chemistry and biophysical variables. The objective of the present study was to assess the influence of NPV and forest structure on the determination of leaf chlorophyll concentration from synthetic reflectance

* Corresponding author.

measurements. The exploitation of the theoretical data may lead to *Cab* retrieval feasibility maps concerning plausible canopy structural configurations that may potentially take place during forest aging.

2. METHODOLOGY

2.1 Radiative transfer models: PROFLIGHT

During development stages in natural forest series two irreversible processes take place during forest aging: 1) Stands become woodier. This is particularly the case once reaching the status of 'old-growth' where masses of coarse woody debris propagate throughout the canopy. And: 2) the spatial arrangements of woody elements and green foliage become heterogeneously distributed in vertical and horizontal dimension (Franklin et al. 2002).

To study the perturbing effects of woody elements (NPV) in the retrieval of *Cab* content for any canopy plausibly to occur during development stages on the basis of synthetic data, a leaf optical properties model (PROSPECT) was coupled with a 3-D canopy model (FLIGHT). PROSPECT idealizes the leaf as a pile of elementary plates composed of absorbing and diffusing constituents. The version of the model used here (Jacquemoud et al., 2000) is parameterized by chlorophyll concentration, the dry matter content, leaf water content, and the effective number of leaf layers. At canopy level, the bidirectional reflectance factor (BRF) for coniferous canopies was computed by the Forest LIGHT interaction model (FLIGHT). FLIGHT allows an explicit representation of complex canopy structures and a correct treatment of crown overlapping and multiple scattering within the scene. In the single crown envelopes foliage is approximated by statistical foliage properties with optical properties of both leaf (PV) and woody phytoelements (NPV). The canopy is (lower) bounded by a soil medium with anisotropic scattering functioning according to Hapke (1981). The horizontal exchange of rays with neighboring areas is arranged by cyclic boundary conditions, meaning that laterally exiting rays of the bounding box are re-cast from the opposite plane at the same trajectory angle to extend scattering to an infinitely extended forest. Subsequently, each generated scene canopy reflectance is the result of a unique, plausible, stand configuration.

2.2 Study sites

The models are parameterized based on field data from an old-growth coniferous forest in Swiss National Park (SNP), Switzerland (10°13′48″E/46°39′45″N). SNP is one of the few areas in Western Europe that was not influenced by humans during most of the 20th century. The forest, characterized by its advanced age (165-200 yr; Cherubini et al., 2002) of the pine stands (*P. montana* and *P. cembra*), is classified as woodland associations of *Erico-Pinetum mugo* (Zoller, 1995). The overstory canopy is typified by relatively open and discontinuous stands resulting in a relatively low Leaf Area Index (LAI; between 1.5 and 4.5, Kötz et al., 2004) and a high fraction of total woody parts (e.g. trunks, branches, standing and fallen deadwood).

Further, to exemplify the theoretical results into the context of real-world forests one young and two mature coniferous stands were additionally selected:

Young Norway spruce: This Norway spruce (*Picea abies* (L.) Karst.) stand is located in the Moravian–Silesian Beskydy Mountains, in the eastern part of the Czech Republic bordering with Slovakia (49°50' N, 18°54' E). The trees of the monoculture plantation are currently 30 years old. Foliage is concentrated in the dense, uniform overstory, characterized by a mean canopy LAI of 7.8 and a mean canopy cover of 82%. (Homolová et al., 2007).

Early mature Lodgepole pine: This Lodgepole pine (*Pinus contorta*) stand is located in the central interior of British Columbia, Canada. The ecosystem in this area is dominated by the Sub-Boreal Spruce (SBS) biogeoclimatic zone. The forest is located approximately in the centre of the province (124° 18' N, 53° 39' E) and is between 61-80 years old. The region is attacked by mountain pine beetle since the mid nineties. Coarse–resolution LAI maps (Chen et al., 2002) indicate that LAI of this region ranges between 4 and 5. Crown coverage is visually assessed to range between 60 and 80%.

Mature forest Norway spruce: This Norway spruce stand is located in the Sumava Mountains, (Bohemian Forest, southern Czech Republic; 48° 59' N, 13° 28' E). The region holds some of the best preserved and least human-influenced spruces forests in Central Europe. The age of the stand is over 100 (±125) years (Wild et al., 2004). An extensive area of Norway spruce was affected by a massive bark beetle outbreak since the mid-1990s whereby vast stands lost all their needles (grey-attack) (Jonášová & Prach, 2004).

2.3 Optical properties

The investigation of confounding factors affecting the relationship between reflectance and *Cab* requires the simulation of many reflectance spectra, at needle-level and canopy-level. At needle level, it is well known that needle chlorophyll concentration depends on age of needles (Jach & Ceulemans, 2000), stress (Carter & Knapp, 2001) and location within the canopy. Optical properties of needle leaves were simulated with PROSPECT whereby a variation of *Cab* content was explicitly accounted for. Chosen chlorophyll content ranged from 15 to 95 µg/cm^2 with steps of 10 µg/cm^2. This is a range that may typically occur in a conifer stand.The remaining model variables, leaf mesophyll structure, dry matter and water content were empirically acquired during the Fire Spread and Mitigation (SPREAD) campaign as described in Kötz et al., (2004) and were subsequently aggregated to obtain values generic for the SNP study site (N: 3.80, C_d: 0.036 g/cm^2 and C_w: 0.044 g/cm^2 respectively). Optical properties of the understory background of SNP can be essentially conceptualized as a mixture of PV (shrubs, herbaceous species) and NPV (woody parts, litter) elements; spots of bare soil are virtually absent within the forest. Field spectroradiometric measurements of understory vegetation were aggregated (35 vegetated understory spectra, 10 bark spectra) to approximate the spectral diversity characterizing the background spectra (figure 3a). Further, aggregation of the bark spectra equally led to a generic NPV signature.

From the set of PROSPECT-generated spectra, the average (μ) and associated variation expressed by the standard deviation (σ), was calculated and shown in figure 1a. In a sense, the average of the reflectance series associated with the *Cab* range approximates the reflectance values of a needle with an intermediate chlorophyll concentration (e.g. around 55 µg/cm^2). The figure clearly demonstrates that the influence of chlorophyll concentration is restricted to the visible region and the red edge, with greatest SD (2.69) around 710 nm. Next, to gain insights in the dynamics of the chlorophyll-generated variability, the Coefficient of Variation (*CV*) was calculated:

$$CV_{Cab} = \frac{\sigma}{\mu}, \quad (1)$$

The CV_{Cab} is a useful statistic for comparing the degree of dispersion, from one data series to another, even if the means are drastically different from each other. Figure 1b shows the CV_{Cab} of the PROSPECT-generated spectra with varying chlorophyll content. The derived CV_{Cab} is characterized by a peak in the red edge at 710 nm, which is the response of chlorophyll *a* absorption.

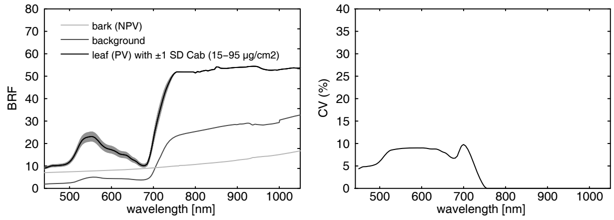

Figure 1. a) Averaged reflectance of a PROSPECT-simulated needle, understory and bark representing the spectral properties of PV, background and NPV relevant for FLIGHT parameterization. The grey band represents the interpolated SD related to the Cab range. b) associated CVCab

2.4 Generation of FLIGHT data set

Variable	Unit	Generic field observations	Range of variation LUT Min	Max	step
Within-crown					
NPV-PV[a]	%	0.7	0.2	1.0	0.1
Crown LAI	-	2.5	1	10	0.5[b]
CC	%	0.6	0.2	0.80	0.1
LAD		Spherical			
Stand structure					
Tree height	m	11.93 ± 2.9			
Crown radius	m	0.88			
Trunk height	m	7.0			
Trunk diameter	m	0.179 (at ground)			

Table 1. Ranges of within-crown structural variables for generation of LUT and field observations of stand variables relevant for FLIGHT parameterization (a: NPV=1-PV; b: 0.5 until LAI: 5 then steps of1.0.). LAD: leaf angle distribution.

Having introduced spectral variability at needle level, the analysis shifts to canopy level through coupling with FLIGHT. Automatic simulations were realized based on Look Up Tables (LUT). Prior to configuring the look-up tables, it is of importance that the relationship between confounding factors (e.g. structure, woody elements) and chlorophyll content is established for any given canopy structure or composition that may occur during a development phase. Key biophysical components that vary throughout stand development were selected, being canopy LAI, crown coverage (CC) and, to accommodate for a varying canopy composition, within-crown NPV and PV proportions. We used collected stand architectural data (e.g., trunk height, tree height, trunk radius, and crown radius) from the SPREAD campaign to parameterize FLIGHT. Their major characteristics are summarized in table 1. The simulated stands were horizontally distributed on a flat terrain according to a Poisson distribution with crowns of irregular conical shape and cylindrical trunks. Within the individual crows a spherical leaf angle distribution of the phytoelements was assumed. Additional parameters were fixed to model default or field measurement as described in Kötz et al. (2004).

Canopy reflectance was simulated as observed from nadir in 18 spectral bands corresponding with specifications of CHRIS in Mode 3 (land). CHRIS aboard PROBA (Project for On-board Autonomy) satellite is an experimental smallsat that has the capability to provide combined hyperspectral and multidirectional sampling with high spatial resolution (~17 m) of selected terrestrial targets (Barnsley et al., 2004). In the 'land' mode wavebands are selected specifically to monitor vegetation cover. The spatial size of a CHRIS pixel precisely matched to the FLIGHT scene dimensions (17 m). The solar angle was set as during CHRIS-PROBA overpass over Swiss National Park on 2004-06-27 (θ_s: 24.0°, ϕ_s: 162.8°, see Verrelst et al., 2008 for details). All spectral data were convolved to CHRIS using the CHRIS band centers and full-width-half-maxima (FWHM).

To make sure that explicitly relationships between reflectance spectra and chlorophyll content are studied with no other influencing factors than canopy structure and woody elements, only the vegetation signal free of any contamination is needed. To achieve uncontaminated reflectance spectra, a solution is to apply a total correction for background signal by setting the background layer equivalent to a perfect absorber canopy background condition. In this case the optical characteristics and associated *Cab* range of the experimental overstory canopy signal was directly linked with biophysical parameters, without any atmosphere or background contamination. Once the initialization was done, one million rays penetrated in each experimental canopy. Finally a total of 7938 forest scene simulations (9 *Cab* × 14 crown LAI × 9 NPV-PV × 7CC) executed by PROFLIGHT provided the spectral sampling for the subsequent analysis of the contribution of woody elements and needle *Cab* content at stand level.

3. RESULTS

In FLIGHT, the radiant fluxes interacted with the woody elements and the chlorophyll-containing foliage which resulted into upscaled chlorophyll-induced spectral response. The averaged BRF ($\overline{BRF}$) and chlorophyll-induced spectral dispersion (CV_{Cab}) was once more calculated, now at stand level. Figure 2a and 2b shows the averaged BRF and associated CV_{Cab} for the CHRIS bands and the SNP structural configurations (table 1). With a perfect absorbing background, only the scattering caused by the overstory canopy attributes that escapes into nadir direction are detected. This assures an explicit connection with the structural configurations but, in turn, also leads to low $\overline{BRF}$. Considering the CV_{Cab}, a shape similar to leaf level appeared but then with a markedly higher magnitude (around 35-40%), which can be fully explained by absence of any other confounding factor.

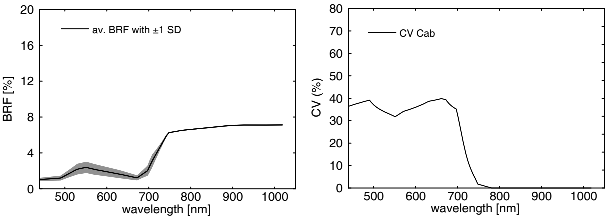

Figure 2. a) $\overline{BRF}$ with interpolated *Cab*-induced SD (grey band). b) associated CV_{Cab} at canopy level as simulated by FLIGHT (crown LAI: 2.5; PV: 70%; CC: 60%).

To exploit the propagated variability along gradients of canopy variables, we chose one specific wavelength where the subtle *Cab* signal is prominently expressed. Wavelengths associated with chlorophyll content are to be found in the 550 or 700 nm regions, where higher contents of chlorophyll *b* and chlorophyll *a*, respectively, are required to saturate the absorptance (Thomas & Gausman, 1977). CHRIS wavebands associated with these chlorophyll regions are λ_{mid}: 530, 551, 570 and 697, 703, 709 nm respectively. For each of these wavebands the CV_{Cab} were plotted along the NPV-PV gradient. The gradient starts from 0% NPV onwards whereby the proportion of canopy woody elements (NPV) gradually increases (figure 3). From this set of chlorophyll-sensitive wavebands, the λ_{mid} 531 nm band exhibited greatest decrease all along the NPV gradient implying greatest sensitivity to woody elements, while the λ_{mid} 709 nm band gave sign of a flatter response implying certain robustness to woody elements. Since apart of chlorophyll, anthocyanin also absorbs around 550 nm (Sims et al., 2002), we opted to continue working with the radiant flux at 709 nm.

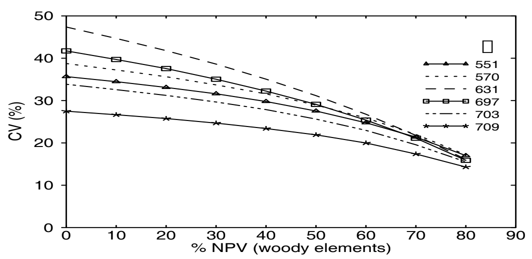

Figure 3. Waveband-dependent trends of CV_{Cab} (%) along the NPV gradient (%PV= 100-%NPV). Values were averaged over the gradients of crown LAI and crown closure.

3.1 Detectability of chlorophyll content

The applicability of observed trends in the context of real-world canopies is analyzed next. As pointed out above, woody parts can significantly govern the canopy cover of coniferous forests. Being aware of varying NPV fractions at sub-pixel level the underlying idea of this modelling exercise is that modelling results may provide canopy-specific indicators regarding the suitability of retrieving chlorophyll content from reflectance data. The Standard deviation (SD) indicates the absolute spread of the reflectance spectra. Due to the fixed *Cab* range the magnitude of the SD is explicitly governed by structural attributes. Consequently, given the assumption that a greater spectral spread allows easier detection and mapping of chlorophyll content, the SD results provides thus a theoretical indicator of the stand-dependent chlorophyll content detectability. To exemplify this, four structurally distinct real-world forests were selected (figure 4).

Each of the coniferous stands holds near-optimal conditions to retrieve chlorophyll content in terms of CC and crown LAI with the exception of the heavily affected spruce stand in the Sumava Mountains. They encompass a CC of 60% or higher and a varying crown LAI. The homogenous, dense young spruce stand (figure 4a), for example, is characterized by high crown LAI value (7.8) which results into a slight suppressed SD as a consequence of the LAI-dependent chlorophyll absorptions. The other test sites encompass a lower LAI which implies a slightly greater spectral spread and thus detectability.
When positioning the four stands along the NPV-PV gradient, however, only then the true *Cab* detection feasibility appears. The virtual absence of woody cover in the outer canopy of the young spruce stand implies that the full *Cab*-related variability can reach a sensor without any contamination. Canopy structure such as the high LAI would be the limiting factor here, but only to a minor extent (figure 4e). By contrast, the old-growth forest in SNP gave sign of a more complicated canopy structure and composition (figure 4b). As a consequence of dead and partly dead trees a fractional NPV cover may reach up to 30% at CHRIS pixel resolution. Due to the scattered woody parts within the canopy, PV and NPV of this stand are heterogeneously arranged in a quasi-random manner. The modeling results indicate that such woody contribution may suppress the chlorophyll-dependent spectral spread with 28% given the SNP structural configurations (CC: 0.60; LAI: 2.5). However, note that the canopy throughout the test site is rather open meaning that in reality understory, which is again a mixture of PV and NPV, will partly contribute to the chlorophyll signal as well.

Contrarily to the latter, the infested stands in British Columbia (figure 4c) and in the Bohemian Forest (figure 4d) are from another order of woodiness. The British Columbian stand shows mixtures of green trees, red-attack trees and grey-attack trees throughout the forest (figure 4d). Subsequently, the spatial distribution of NPV fractional cover varies dramatically. Such spatial PV-NPV variation implies that relationships between reflectance spectra and the needle pigment concentrations of remaining foliage are perturbed in a pixel-specific way. The presented results of the rapid declining SD along the NPV-PV gradient indicate the magnitude of change (figure 4f, g). Finally, the example of the Bohemian Forest reflects the worst case situation: virtually the complete stand suffers from insect defoliation. Only small patches and a few isolated trees are left unaffected. What is left of the signal from remaining green cover is in consequence heavily suppressed by dominating NPV cover. No structural assessments have been carried out in this region. With a visually assessed of remaining 40% PV and 50% CC the modeling results indicated that only 58% of the full *Cab* spread is left over.

4. CONCLUSIONS

Natural forests go through development stages with increasing heterogeneity in the distribution of foliage and woody parts. The direct observable effects of these trajectories are that structural variables such as fractional cover, LAI and the amount and arrangement of woody elements alter over time. For instance, the old-growth forest of Swiss National Park that for a long time suffers from severe Alpine conditions (wind, ice and snow storms) and root-rot fungi is gradually reshaped into a highly heterogeneous, woody forest. Furthermore, examples of mature forests prone to insect defoliation demonstrate that woody parts may dominate the canopy cover already earlier in the development phases coniferous canopies (e.g. Radelhoff et al., 1999).

Needle chlorophyll content of these forests can be detected and mapped by fine-resolution satellites such as CHRIS-PROBA. Further, it has been demonstrated (Rautiainen et al., 2008; Verrelst et al., 2008) that CHRIS data with its relatively small pixel resolution (~17.0 m) matches well with radiative transfer models that provide scene-based BRF data of stands.

Modeling results without background contamination demonstrate that nearly all real-world structural features match to quasi-optimal conditions for detecting and mapping chlorophyll from reflectance data as long as the fractional NPV fractional cover is low. In denser canopies a passive sensor cannot penetrate through tree crowns and detect signatures directly under tree canopy so the contribution of a background is of less importance in determining the *Cab*-related spread. In sparse canopies (CC<40%), however, the background signal may either act as an additional distorter (when ground cover is e.g. litter, bare soil) or contribute to the *Cab* variability (when ground cover is e.g. grass, shrubs), or may even be composed in a similar manner as the overstory (e.g. mixture of PV and NPV). The latter is the case in old-growth forests. Conclusively, modeling results demonstrated that canopy composition is the key player in determining the success of *Cab* retrieval. Within the scope of leaf-to-canopy upscaling problem, further efforts should be devoted to the robustness of chlorophyll retrieval techniques, with special attention to correct for fractional wood cover.

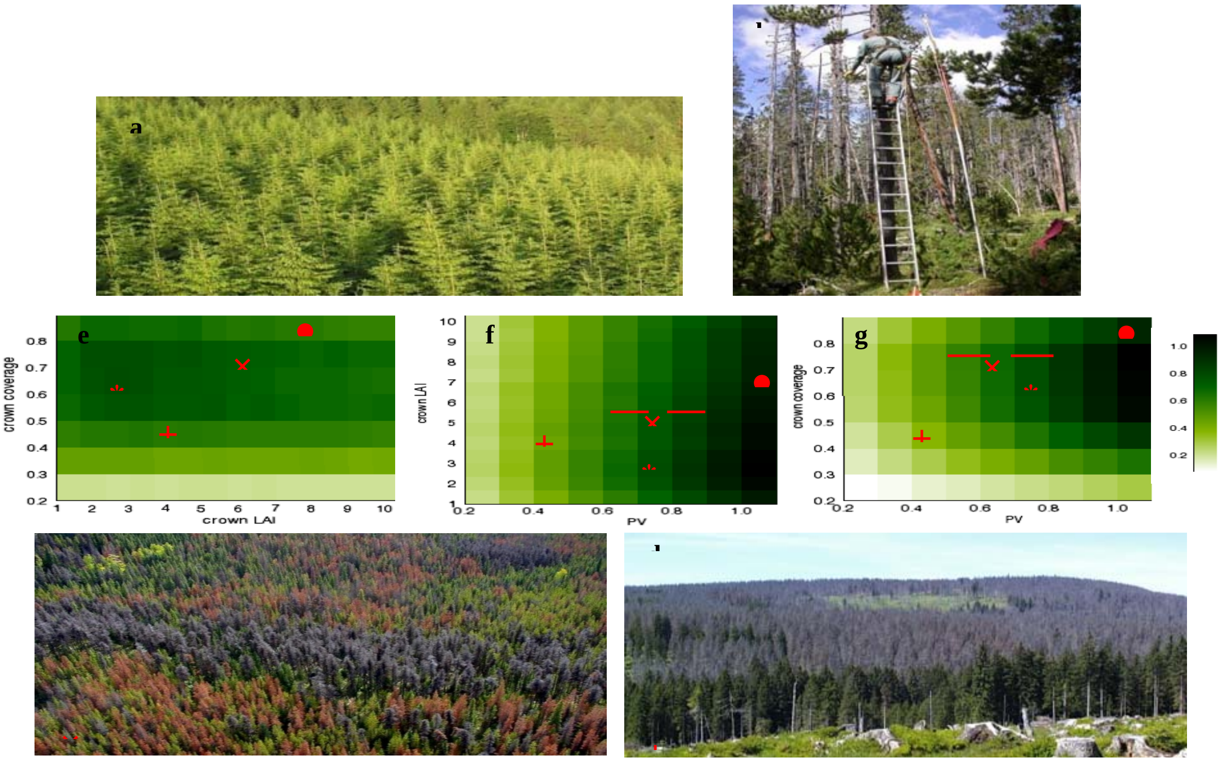

Figure 4. The four study sites (a) young Norway spruce stand, b) old-growth forest, c) early mature beetle-infected lodgepole pine and, d) mature beetle-infected Norway spruce) positioned within the three landscapes of plausible canopies(e: CC vs. crown LAI; f: crown LAI vs. PV; g: CC vs. PV) representing SD. (fixed for e, f, g: CC: 0.60; LAI: 2.5)

ACKNOWLEDGEMENT

The work of J. Verrelst was supported through the Dutch SRON GO programme (Grant-No. EO-080).

REFERENCES

Asner, G.P. 1998. Biophysical and biochemical sources of variability in canopy reflectance. *Remote Sensing of Environment,* 64(3), pp. 234-253.

Asner, G.P., Townsend, A.R., Bustamante, M.M.C., Nardoto, G.B. & Olander, L.P. 2004. Pasture degradation in the central Amazon: Linking changes in carbon and nutrient cycling with remote sensing. *Global Change Biology,* 10(5), pp. 844-862.

Barnsley, M.J., Settle, J.J., Cutter, M.A., Lobb, D.R. & Teston, F. 2004. The PROBA/CHRIS mission: A low-cost smallsat for hyperspectral multiangle observations of the earth surface and atmosphere. *IEEE Transactions on Geoscience and Remote Sensing*, 42(7), pp. 1512-1520.

Bowyer, P. & Danson, F.M. 2004. Sensitivity of spectral reflectance to variation in live fuel moisture content at leaf and canopy level. *Remote Sensing of Environment,* 92(3), pp. 297-308.

Carter, G.A. & Knapp, A.K. 2001. Leaf optical properties in higher plants: Linking spectral characteristics to stress and chlorophyll concentration. *American. Journal of Botany*., 88(4), pp. 67-684.

Chen, J.M., Pavlic, G., Brown, L., Cihlar, J., Leblanc, S.G., White, H.P., Hall, R.J., Peddle, D.R., King, D.J., Trofymow, J.A., Swift, E., Van Der Sanden, J. & Pellikka, P.K.E. 2002. Derivation and validation of Canada-wide coarse-resolution leaf area index maps using high-resolution satellite imagery and ground measurements. *Remote Sensing of Environment,* 80(1), 165-184.

Franklin, J.F., Spies, T.A., Pelt, R.V., Carey, A.B., Thornburgh, D.A., Berg, D.R., Lindenmayer, D.B., Harmon, M.E., Keeton, W.S., Shaw, D.C., Bible, K. & Chen, J. 2002. Disturbances and structural development of natural forest ecosystems with silvicultural implications, using Douglas-fir forests as an example. *Forest Ecology and Management*, 155(1-3), pp. 399-423.

Gitelson, A. & Merzlyak, M.N. 1994. Spectral relfectance changes associated with autumn senescence of Aesculus hippocastanum L. and Acer platanoides L. leaves. Spectral features and relation to chlorophyll estimation. *Journal of Plant Physiology,* 143(3), pp. 286-292.

Jach, M.E. & Ceulemans, R. 2000. Effects of season, needle age and elevated atmospheric CO2 on photosynthesis in Scots pine (Pinus sylvestris). *Tree Physiology,* 20(3), pp. 145-157.

Jacquemoud, S., Bacour, C., Poilve, H. & Frangi, J.P. 2000. Comparison of four radiative transfer models to simulate plant canopies reflectance: Direct and inverse mode. *Remote Sensing of Environment,* 74(3), pp. 471-481.

Jacquemoud, S., Ustin, S.L., Verdebout, J., Schmuck, G., Andreoli, G. & Hosgood, B. 1996. Estimating leaf biochemistry using the PROSPECT leaf optical properties model. *Remote Sensing of Environment,* 56(3), pp. 194-202.

Jonasova, M. & Prach, K. 2004. Central-European mountain spruce (Picea abies (L.) Karst.) forests: Regeneration of tree species after a bark beetle outbreak. *Ecological Engineering*, 23(1), 15-27.

Jia, G.J., Burke, I.C., Goetz, A.F.H., Kaufmann, M.R. & Kindel, B.C. 2006. Assessing spatial patterns of forest fuel using AVIRIS data. *Remote Sensing of Environment,* 102(3-4), pp. 318-327.

Hapke, B. 1981. Bidirectional reflectance spectroscopy. 1. Theory. *Journal of Geophysical Research.,* 86(4 B), 3039-3054.

Homolova, L., Malenovsky, Z., Hanus, J., Tmaskova, I. Dvoorakova, M., Pokorny, R., 2007. Comparison of different ground techniques to map leaf area index of Norway spruce forest canopy. *10th International Symposium on Physical Measurements and Signatures in Remote Sensing, ISPMSRS* 2007, Davos, Switserland, 12.3-14.3.2007

Kötz, B., Morsdorf, F., Itten, K., Schaepman, M., Bowyer, P. & Allgöwer, B. 2004. Radiative transfer modeling within a heterogeneous canopy for estimation of forest fire fuel properties. *Remote Sensing of Environment*, 92(3), pp. 332-344.

Malenovsky, Z., Martin, E., Homolova, L., Gastellu-Etchegorry, J.P., Zurita-Milla, R., Schaepman, M.E., Pokorny, R., Clevers, J.G.P.W. & Cudlin, P. 2008. Influence of woody elements of a Norway spruce canopy on nadir reflectance simulated by the DART model at very high spatial resolution. *Remote Sensing of Environment,* 112(1), pp. 1-18.

North, P.R.J. 1996. Three-dimensional forest light interaction model using a Monte Carlo method. *Ieee Transactions on Geoscience and Remote Sensing*, 34(4), pp. 946-956.

Radeloff, V.C., Mladenoff, D.J. & Boyce, M.S. 1999. Detecting jack pine budworm defoliation using spectral mixture analysis: Separating effects from determinants. *Remote Sensing of Environment,* 69(2), pp. 156-169.

Rautiainen, M., Stenberg, P., Nilson, T. & Kuusk, A. 2004. The effect of crown shape on the reflectance of coniferous stands. *Remote Sensing of Environment,* 89(1), pp. 41-52.

Siitonen, J. 2001. Forest management, coarse woody debris and saproxylic organisms: Fennoscandian boreal forests as an example. *Ecological Bulletins,* 49, pp. 11-41.

Sims, D.A. & Gamon, J.A. 2002. Relationships between leaf pigment content and spectral reflectance across a wide range of species, leaf structures and developmental stages. *Remote Sensing of Environment,* 81(2-3), 337-354.

Song, C. & Woodcock, C.E. 2002. The spatial manifestation of forest succession in optical imagery: The potential of multiresolution imagery. *Remote Sensing of Environment,* 82(2-3), pp. 271-284.

Thomas, J.R. & Gausman, H.W. 1977. Leaf reflectance vs. leaf chlorophyll and carotenoid concentrations for eight crops. *Agronomy Journal*, 69, 799-802.

Trotter, G.M., Whitehead, D. & Pinkney, E.J. 2002. The photochemical reflectance index as a measure of photosynthetic light use of efficiency for plants with varying foliar nitrogen contents. *International Journal of Remote Sensing*, 23(6), pp. 1207-1212.

Ustin, S.L., Roberts, D.A., Gamon, J.A., Asner, G.P. & Green, R.O. 2004. Using imaging spectroscopy to study ecosystem processes and properties. *BioScience,* 54(6), pp. 523-534.

Verrelst, J., Schaepman, M.E., Koetz, B. & Kneubuhler, M. 2008. Angular sensitivity analysis of vegetation indices derived from CHRIS/PROBA data. *Remote Sensing of Environment,* 112(5), pp. 2341-2353.

White, J.C., Wulder, M.A., Brooks, D., Reich, R. & Wheate, R.D. 2005. Detection of red attack stage mountain pine beetle infestation with high spatial resolution satellite imagery. *Remote Sensing of Environment,* 96(3-4), 340-351.